Supporting Information for "Gamma-ray Showers Observed at Ground Level in Coincidence With Downward Lightning Leaders"

R.U. Abbasi[1], T.Abu-Zayyad[1], M. Allen[1], E. Barcikowski[1], J.W. Belz[1], D.R. Bergman[1], S.A. Blake[1], M. Byrne[1], R. Cady[1], B.G. Cheon[4], J. Chiba[5], M. Chikawa[6], T. Fujii[7], M. Fukushima[7,8], G. Furlich[1], T. Goto[9], W. Hanlon[1], Y. Hayashi[9], N. Hayashida[10], K. Hibino[10], K. Honda[11], D. Ikeda[7], N. Inoue[2], T. Ishii[11], H. Ito[12], D. Ivanov[1], S. Jeong[13], C.C.H. Jui[1], K. Kadota[14], F. Kakimoto[3], O. Kalashev[15], K. Kasahara[16], H. Kawai[17], S. Kawakami[9], K. Kawata[7], E. Kido[7], H.B. Kim[4], J.H. Kim[1], J.H. Kim[18], S.S. Kishigami[9], P.R. Krehbiel[19], V. Kuzmin[15], Y.J. Kwon[20], J. Lan[1], R. LeVon[1], J.P. Lundquist[1], K. Machida[11], K. Martens[8], T. Matuyama[9], J.N. Matthews[1], M. Minamino[9], K. Mukai[11], I. Myers[1], S. Nagataki[12], R. Nakamura[27], T. Nakamura[22], T. Nonaka[7], S. Ogio[9], M. Ohnishi[7], H. Ohoka[7], K. Oki[7], T. Okuda[23], M. Ono[24], R. Onogi[9], A. Oshima[25], S. Ozawa[16], I.H. Park[13], M.S. Pshirkov[14,26], J. Remington[1], W. Rison[19], D. Rodeheffer[19], D.C. Rodriguez[1], G. Rubtsov[15], D. Ryu[18], H. Sagawa[7], K. Saito[7], N. Sakaki[7], N. Sakurai[9], T. Seki[27], K. Sekino[7], P.D. Shah[1], F. Shibata[11], T. Shibata[7], H. Shimodaira[7], B.K. Shin[9], H.S. Shin[7], J.D. Smith[1], P. Sokolsky[1], R.W. Springer[1], B.T. Stokes[1], T.A. Stroman[1], H. Takai[29], M. Takeda[7], R. Takeishi[7], A. Taketa[30], M. Takita[7], Y. Tameda[31], H. Tanaka[9], K. Tanaka[32], M. Tanaka[21], R.J. Thomas[19], S.B. Thomas[1], G.B. Thomson[1], P. Tinyakov[14,32], I. Tkachev[15], H. Tokuno[3], T. Tomida[27], S. Troitsky[15], Y. Tsunesada[9], Y. Uchihori[34], S. Udo[10], F. Urban[33], G. Vasiloff[1], T. Wong[1], M. Yamamoto[27], R. Yamane[9], H. Yamaoka[21], K. Yamazaki[30], J. Yang[35], K. Yashiro[5], Y. Yoneda[9], S. Yoshida[17], H. Yoshii[36], Z. Zundel[1]

Contents of this file

1. Tables S1 to S3

2. Figures S1 to S15

---

[1]High Energy Astrophysics Institute and Department of Physics and Astronomy, University of Utah, Salt Lake City, Utah, USA

[2]The Graduate School of Science and Engineering, Saitama University, Saitama, Saitama, Japan

[3]Graduate School of Science and Engineering, Tokyo Institute of Technology, Meguro, Tokyo, Japan

[4]Department of Physics and The Research Institute of Natural Science, Hanyang University, Seongdong-gu, Seoul, Korea

[5]Department of Physics, Tokyo University of Science, Noda, Chiba, Japan

[6]Department of Physics, Kinki University, Higashi Osaka, Osaka, Japan

[7]Institute for Cosmic Ray Research, University of Tokyo, Kashiwa, Chiba, Japan

Introduction

The tables and figures in this supporting document provide further detail on the observations of the Lightning Mapping Array (LMA), Slow Antenna (SA), and Telescope Array Surface Detector (TASD) detectors.

[17]Department of Physics, Chiba University, Chiba, Chiba, Japan

[18]Department of Physics, School of Natural Sciences, Ulsan National Institute of Science and Technology, UNIST-gil, Ulsan, Korea

[19]Langmuir Laboratory for Atmospheric Research, New Mexico Institute of Mining and Technology, Socorro, New Mexico 87801, USA.

[20]Department of Physics, Yonsei University, Seodaemun-gu, Seoul, Korea

[21]Institute of Particle and Nuclear Studies, KEK, Tsukuba, Ibaraki, Japan

[22]Faculty of Science, Kochi University, Kochi, Kochi, Japan

[23]Department of Physical Sciences, Ritsumeikan University, Kusatsu, Shiga, Japan

[24]Department of Physics, Kyushu University, Fukuoka, Fukuoka, Japan

Date	Time	μsec	LMA dBW	NLDN I_{pk}	TASD VEM_{max}/MeV	Number of TASDs
2015/09/15	12:13:04	755191	16.2			
		293	18.0			
		343	15.6			
		413	13.3			
		422		-4.3 kA C		
		558	19.4			
		662	22.2			
		670			30/61	5
		672		-15.5 kA C		
		752	21.4			
		756		-17.5 kA C		
		757			449/920	9
		871			37/55	15
		873		-22.1 kA C		
		939			142/291	8
		950		-15.0 kA C		
		756035		-10.0 kA C		
		065			39/80	8
		260	18.6			
		855	18.6			
		951144		-7.1 kA G		
2015/09/15	19:37:01	821147	14.6			
		339	24.4			
		344		-12.3 kA C		
		450	17.4			
		451		-8.1 kA C		
		564	23.5			
		584		+17.1 kA G†		
		586		+18.4 kA G†		
		633			72/148	8
		643	23.2			
		759	16.6			
		812			75/154	6
		842		+9.3 kA C		
		847			47/96	6
		948			25/51.2	4
		822043	15.7			
		822094		-5.8 kA C		
		172	19.8			
		631	20.1			

Table S1a: Quantitative data for the initial 2 ms of the TGF flashes FL1 and FL2. Shown are the dBW VHF source powers of the detected LMA activity, the peak currents I_{pk} of the NLDN detected events, and the maximum vertical equivalent muon (VEM) strengths of the detected gamma bursts. Horizontal dashed lines separate temporally correlated events. The two daggered (†) NLDN events for FL2 are duplicate detections of a single event, which we deduce from the LMA observations is a misidentified +IC rather than a +CG.

[25]Engineering Science Laboratory, Chubu University, Kasugai, Aichi, Japan

[26]Sternberg Astronomical Institute Moscow M.V.Lomonosov State University, Moscow, Russia

[27]Department of Computer Science and Engineering, Shinshu University, Nagano, Nagano, Japan

[28]Department of Physics and Astronomy, Rutgers University - The State University of New Jersey, Piscataway, New Jersey, USA

[29]Brookhaven National Laboratory, Upton, New York, USA

[30]Earthquake Research Institute, University of Tokyo, Bunkyo-ku, Tokyo, Japan

[31]Department of Engineering Science, Faculty of Engineering, Osaka Electro-Communication University, Neyagawa, Osaka, JAPAN

[32]Graduate School of Information Sciences, Hiroshima City University, Hiroshima, Hiroshima, Japan

[33]Service de Physique Theorique, Universite Libre de Bruxelles, Brussels, Belgium

[34]National Institute of Radiological Science, Chiba, Chiba, Japan

[35]Department of Physics and Institute for the Early Universe, Ewha Womans University, Seodaaemun-gu, Seoul, Korea

[36]Department of Physics, Ehime University, Matsuyama, Ehime, Japan

[8]Kavli Institute for the Physics and Mathematics of the Universe (WPI), Todai Institutes for Advanced Study, the University of Tokyo, Kashiwa, Chiba, Japan

[9]Graduate School of Science, Osaka City University, Osaka, Osaka, Japan

[10]Faculty of Engineering, Kanagawa University, Yokohama, Kanagawa, Japan

[11]Interdisciplinary Graduate School of Medicine and Engineering, University of Yamanashi, Kofu, Yamanashi, Japan

[12]Astrophysical Big Bang Laboratory, RIKEN, Wako, Saitama, Japan

[13]Department of Physics, Sungkyunkwan University, Jang-an-gu, Suwon, Korea

[14]Department of Physics, Tokyo City University, Setagaya-ku, Tokyo, Japan

[15]National Nuclear Research University, Moscow Engineering Physics Institute, Moscow, Russia

[16]Advanced Research Institute for Science and Engineering, Waseda University, Shinjuku-ku, Tokyo, Japan

Date	Time	μsec	LMA dBW	NLDN I_{pk}	TASD VEM_{max}/MeV	Number of TASDs
2016/05/10	02:41:50	846823	-5.9			
		932	9.5			
		847017	19.1			
		141	15.1			
		267	15.1			
		467	22.8			
		527	20.8			
		606	25.2			
		706	17.2			
		713		-7.3 kA C		
		987	15.1			
		848132	19.0			
		208	20.0			
		299	13.8			
		434	15.4			
		643	16.8			
		708	11.8			
		761	16.5			
		910			105/215	6
		849035			109/223	6
		248			4,162/8,532	4
		342			22,118/45,342	4
		368		-94.1 kA G		
		637	14.9			

Table S1b: Quantitative data for the initial 2 ms of the TGF flash FL3. Shown are the dBW VHF source powers of the detected LMA activity, the peak currents I_{pk} of the NLDN detected events, and the maximum vertical equivalent muon (VEM) strengths of the detected gamma bursts.

Date	Time	μsec	NLDN I_{pk}	TASD VEM_{max}/MeV	Number of TASDs
2014/08/23	13:17:24	286696	-18.8 kA G‡		
		286708		17/35	8
		286970		38/78	5
		315213	-12.2 kA G		
		413879	-8.7 kA G		
2014/09/05	09:47:17	796224		997/2,044	6
		775		450/922	6
		797394	-139.8kA G		
		816052	-5.6 kA C		
		824498	-34.6 kA G		
		841029	-36.9 kA G		
		852938	-7.6 kA G		
		862402	-17.4 kA G		
		060874	-13.2 kA G		
2014/09/05	09:54:07	265892		69/141	9
		963	+32.7 kA C		
		979		701/1,437	11
		267358	-101.1 kA G		
		286098	-24.7 kA G		
		301314	-31.8 kA G		
		325714	-45.0 kA G		
		345298	-8.7 kA G		
2014/09/05	10:05:41	966105	-16.5 kA C		
		967003		57/117	4
		144		78/159	8
		970258	-66.6 kA G		
		988290	-4.8 kA G		

Table S2: Same as Table S1, except for SA-associated flashes FL4 - FL7. We deduce from the SA data that the NLDN event indicated with a double-dagger (‡) is a misidentified −IC rather than a −CG.

Date	Time	μsec	NLDN I_{pk}	TASD VEM_{max}/MeV	Number of TASDs
2014/09/27	07:54:35	496139		285/584	10
		185		187/383	11
		250	-36.8 kA C		
		257		12/25	5
		368		138/283	7
		424		87/178	9
		509971	-11.7 kA G		
		586685	+7.1 kA C		
		602118	-17.6 kA G		
2014/09/27	11:13:48	516097		20/41	4
		193		75/154	5
		258	+15.2 kA C		
		273	-18.4 kA C		
		281		193/396	7
		525789	-16.1 kA G		
		558788	-15.8 kA G		
		575226	-12.3 kA G		
2014/09/27	15:12:54	744882		49/100	7
		961	-15.6 kA C		
		745070		47/96	5
		145		73/150	6
		268	+16.7 kA G†		
		289		49/100	7
		360		47/96	5
		749665	-35.0 kA G		
		777174	-11.8 kA G		
		779576	-13.6 kA C		
		851375	-9.1 kA C		

Table S3: Same as Table S2, except for flashes FL8 - FL10. The daggered (†) NLDN event for FL10 is a misidentified +IC rather than a +CG.

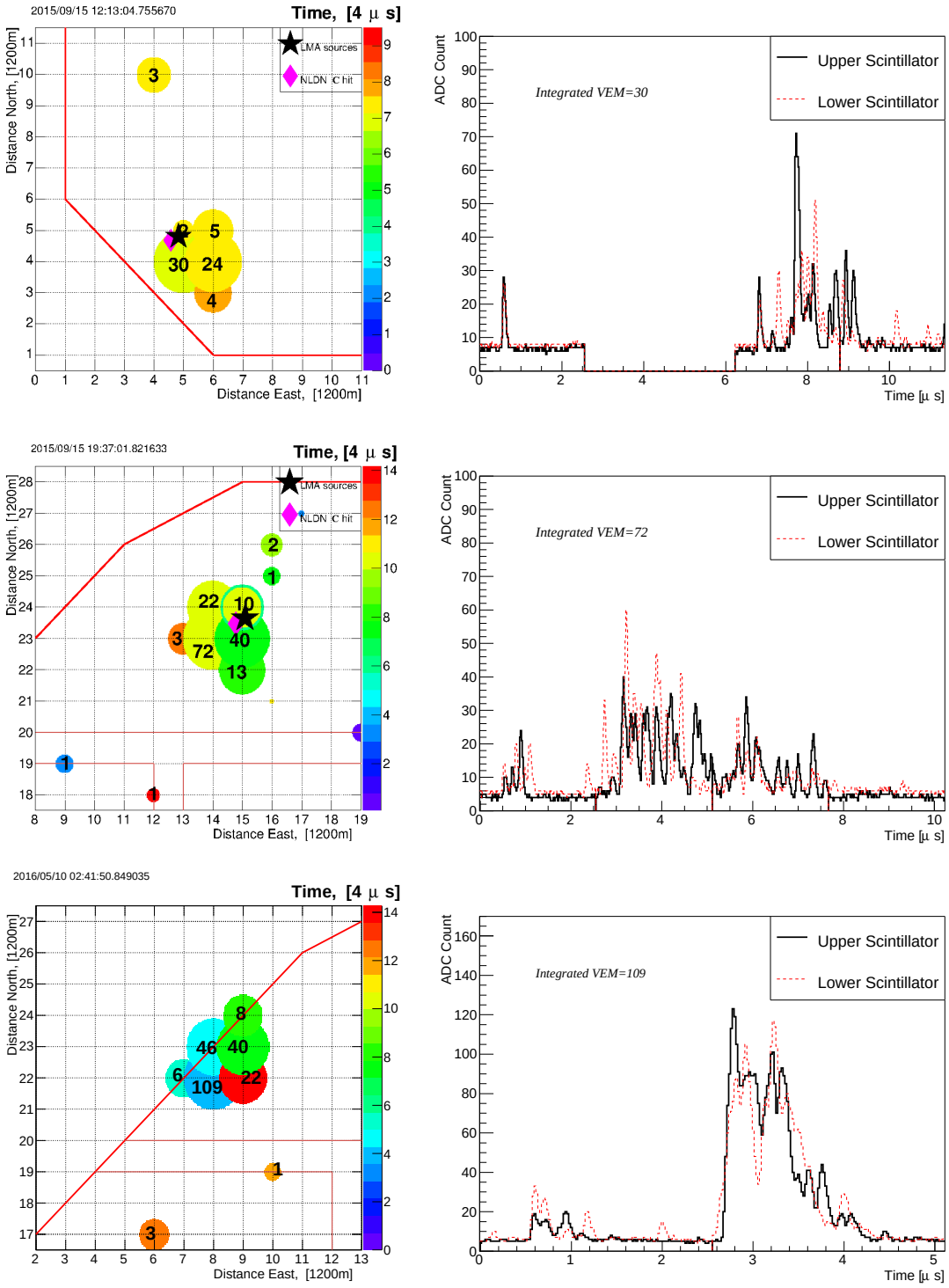

Figure S1: On the left are Footprints of TASD triggers for the LMA-correlated events of Table S1, with the numbers indicating the Vertical Equivalent Muon (VEM) counts (see paper), and the color indicating the relative arrival times. Initial LMA and NLDN events are indicated by stars and diamonds respectively. The red line indicates the boundary of the TASD array. On the right are the upper and lower scintillator waveforms for the TASD triggers for one of SDs in the footprint with the corresponding integrated VEM number.

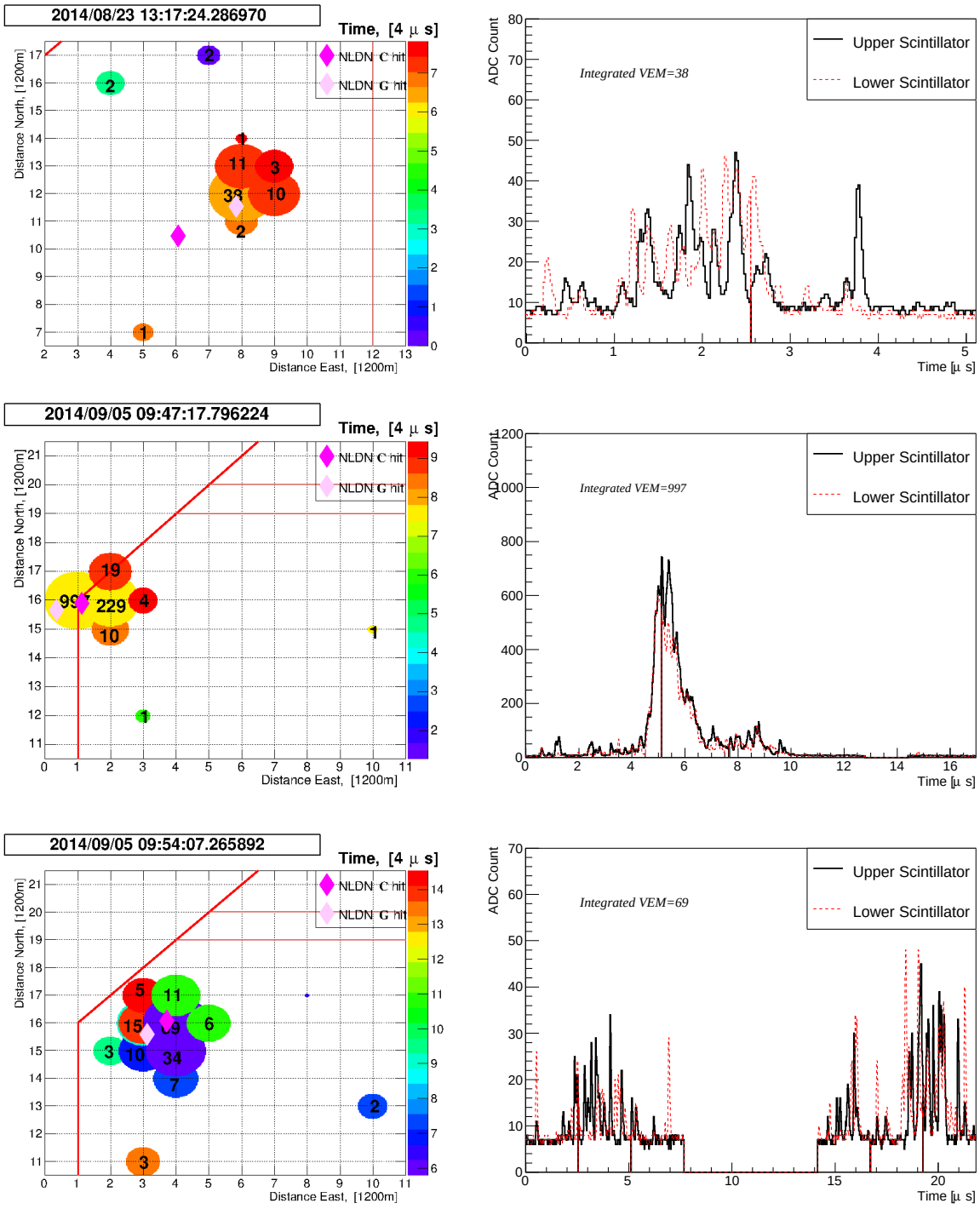

Figure S2: Same as Figure S1, except showing footprints and waveforms for flashes FL4, 5, and 6 of the SA-correlated events of Table S2.

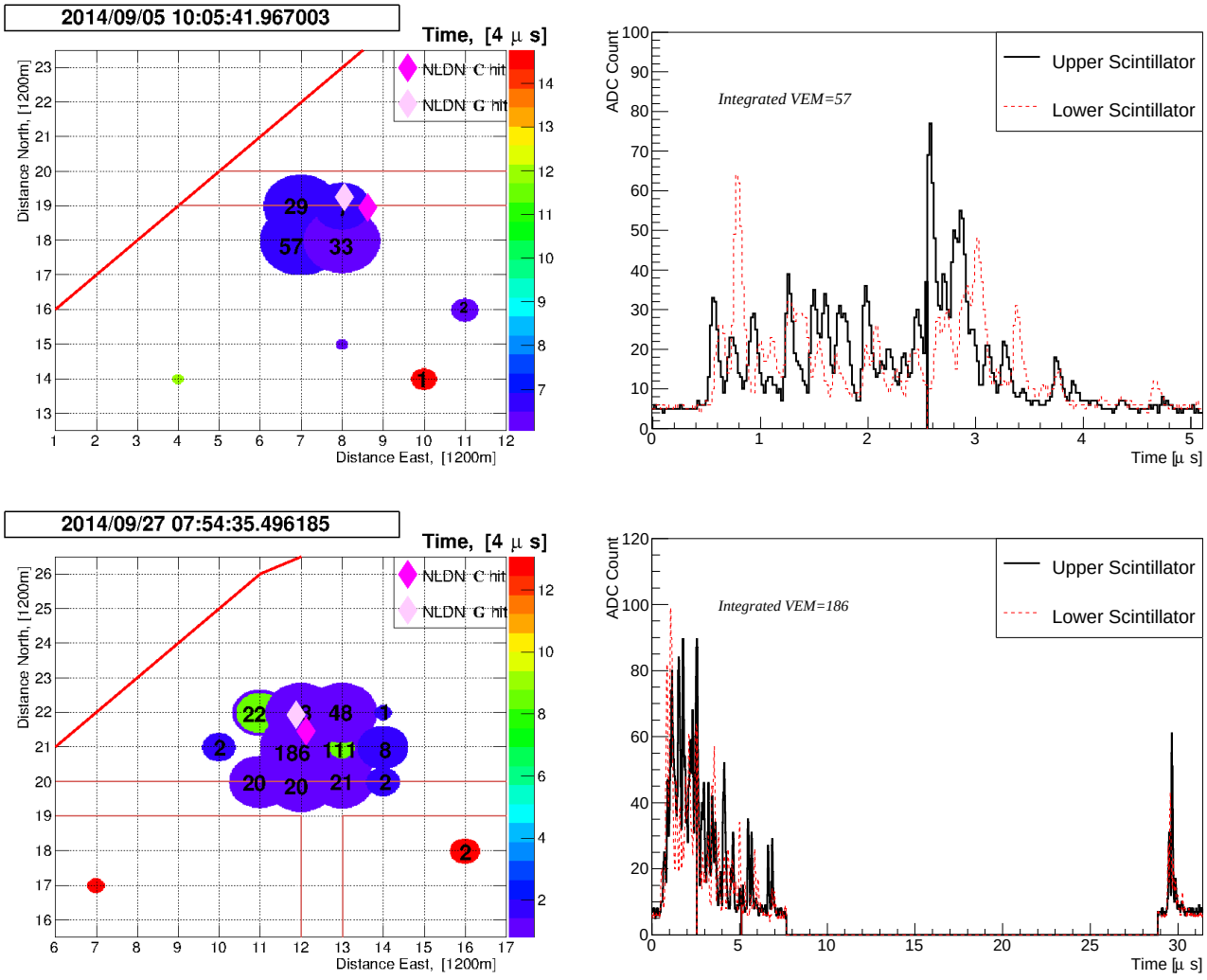

Figure S3: Same as Figure S2, except for flashes FL7 and 8 of the SA-correlated events of Tables S2 and S3.

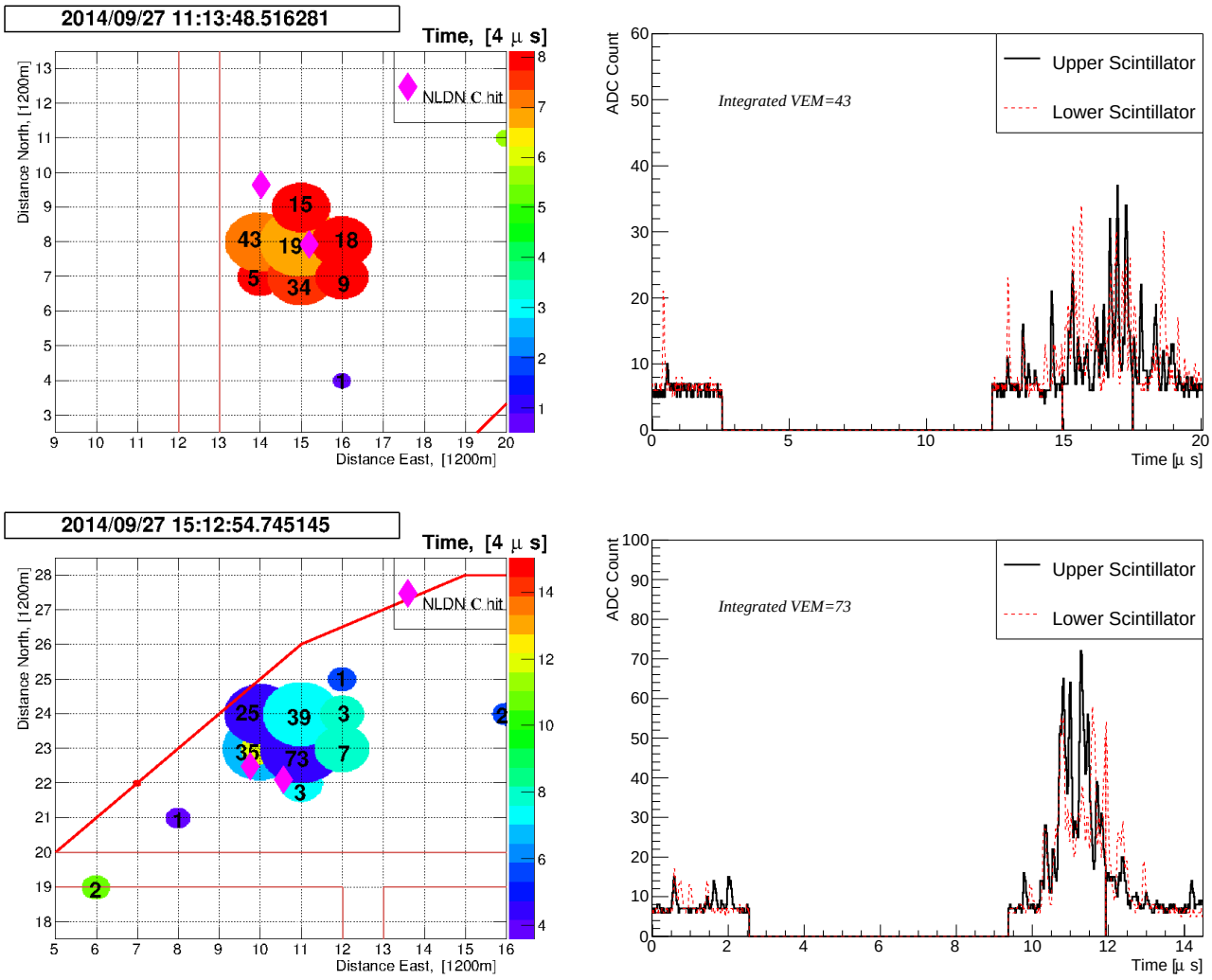

Figure S4: Same as Figure S2, except for flashes FL9 and 10 of the SA-correlated events of Table S3.

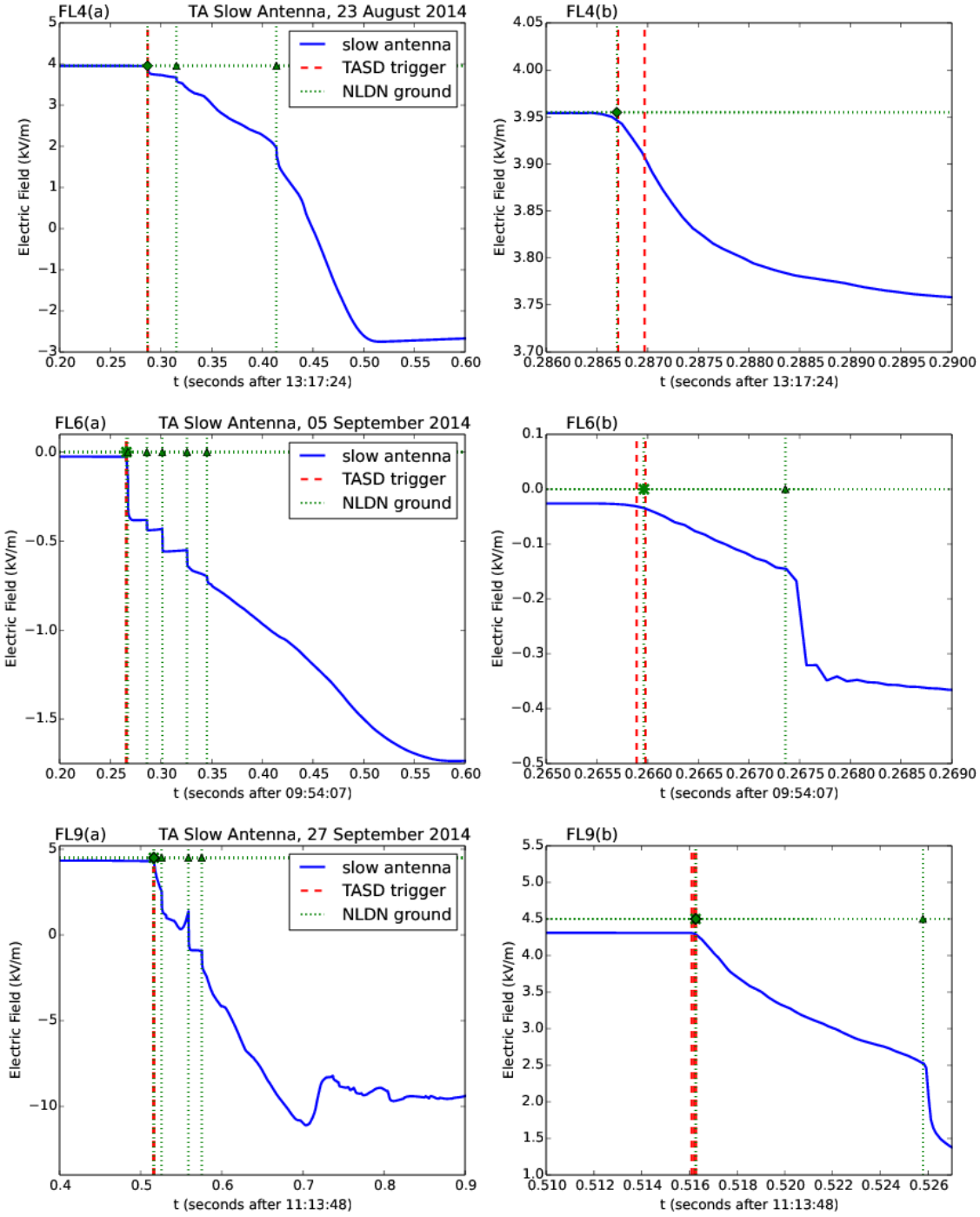

Figure S5: Electric field change versus time for three of the slow-antenna correlated trigger burst events (Flashes 4, 6 and 9). The dashed red lines show the TASD trigger times, while the dot-dashed lines and green symbols indicate the times and type of NLDN events ($\triangle$, $\diamond$, $\times$, $*$ = –CG, –IC, +CG, +IC, respectively). The long negative field changes at the end of flashes are continuing current discharges to ground. The left side panels show the entire flash, while the right side panels zoom in on the initial several ms of the flash.

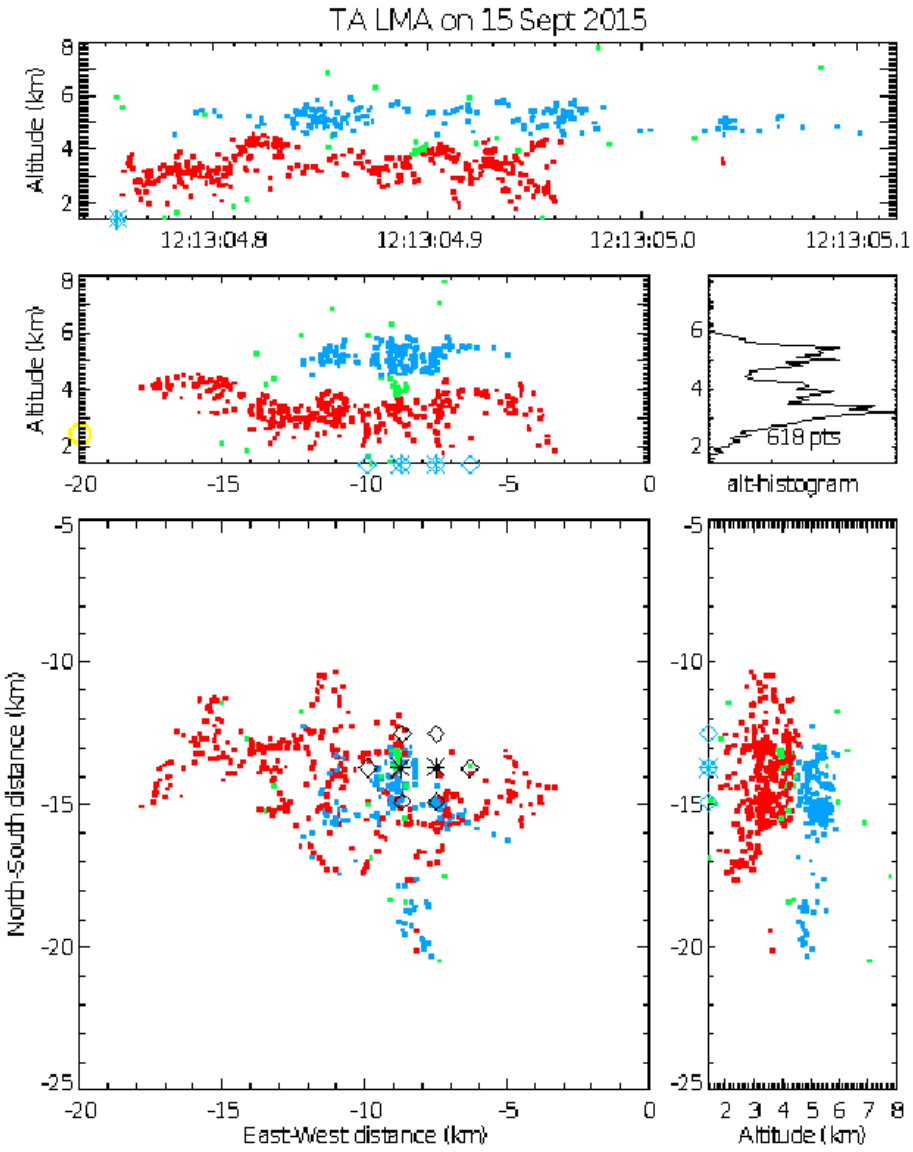

Figure S6: LMA observations of FL1 at 12:13:04 on 15 Sept. 2015, showing where the discharge propagated through negative storm charge between 4.5 and 6 km MSL altitude (blue sources) and lower positive charge at 2.5-4.5 km altitude (red sources). The flash initiated between about 5 and 6 km altitude and developed downward into the lower positive charge, where it continued as a low-altitude intracloud (IC) flash for 200 ms before producing a negative stroke to ground. The diamond and asterisk symbols indicate TASD stations that triggered on the particle shower, with the asterisks indicating the stronger events, and correspond to the footprint of the first flash in Figure S1. In both figures, the event being displayed is the second of five triggers shown in Table S1. Ground is at 1.4 km altitude, corresponding to the lower axis of the height-time and vertical projection panels. The green sources are either noise-affected solutions or indicative of propagation between or outside of the charge regions.

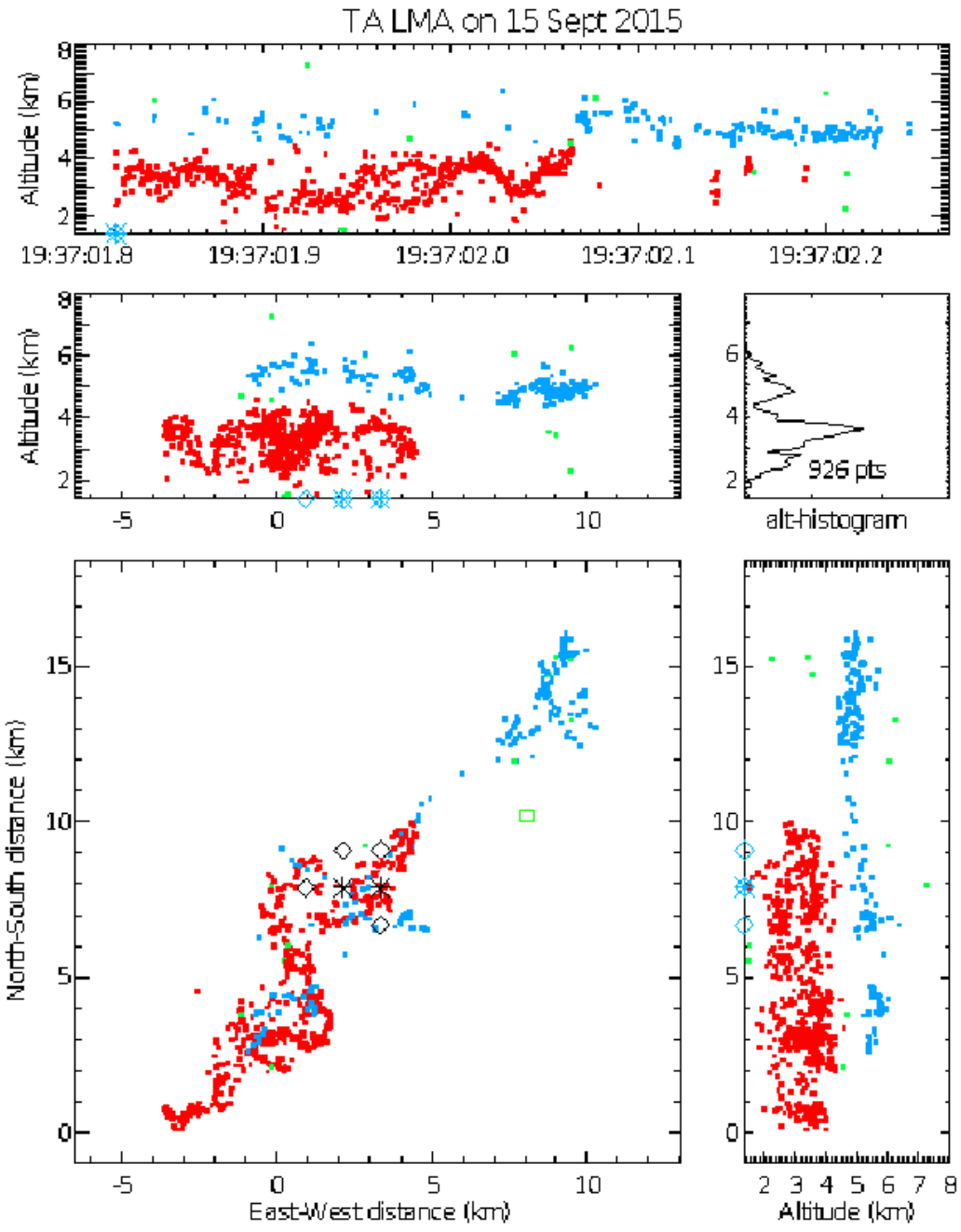

Figure S7: Same as Figure S6, except for FL2 at 19:37:01 on 15 Sept. 2015 (second flash in Figure S1). In this case, the event was the first trigger seen in Table S1.

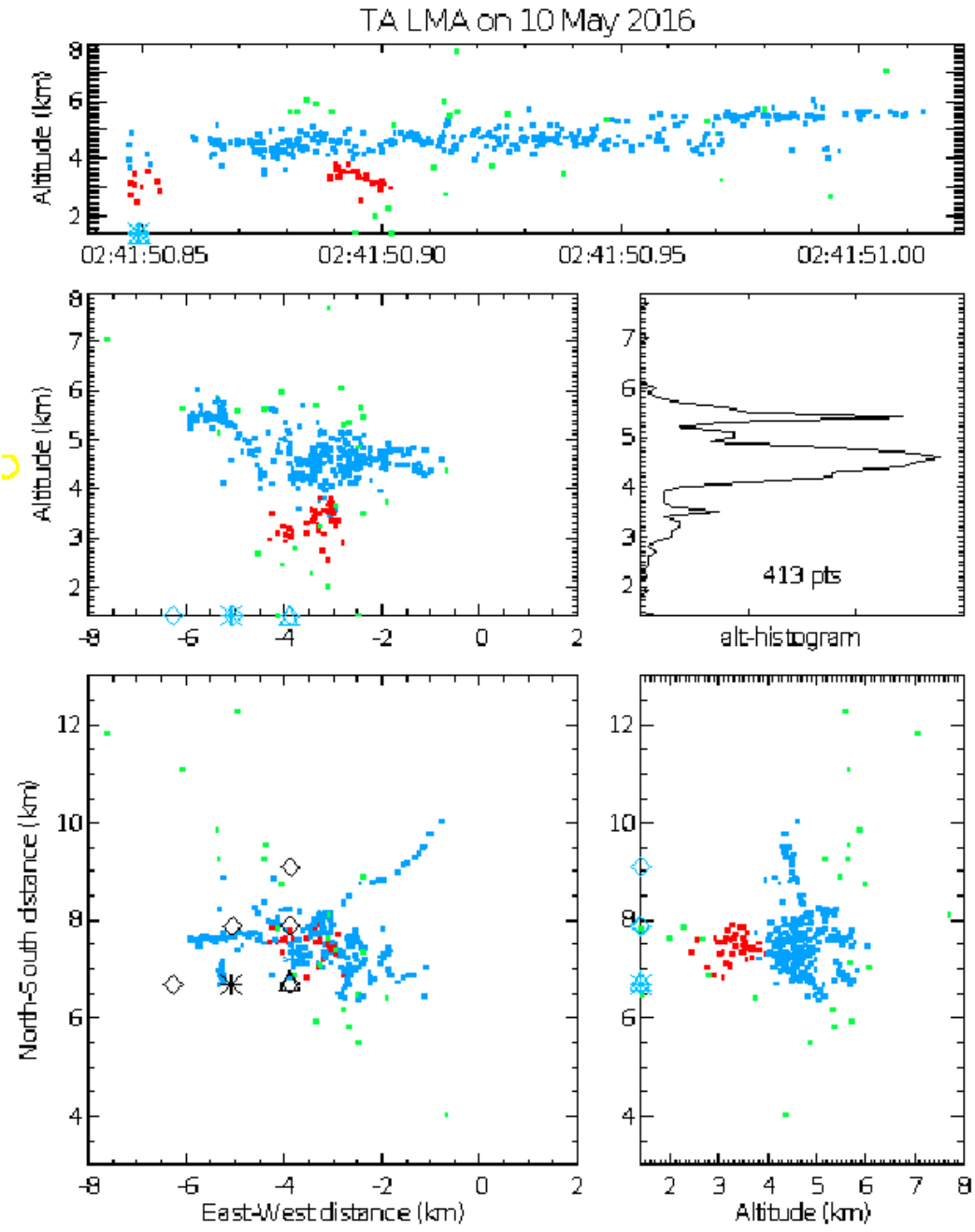

Figure S8: Same as Figure S6, except for FL3 at 02:41:50 on 10 May 2016 (third flash in Figure S1). The flash began with a short-duration (2.6 ms) leader that went quickly to ground (see discussion in main text). From the NLDN data, the leader contacted ground within about 100 m of the southeastern-most TASD station shown in the plan plot (overlapping triangle and diamond symbols). The event being displayed is the second of four triggers that occurred in the final stages of the leader, 333 μs before reaching ground (Table S1).

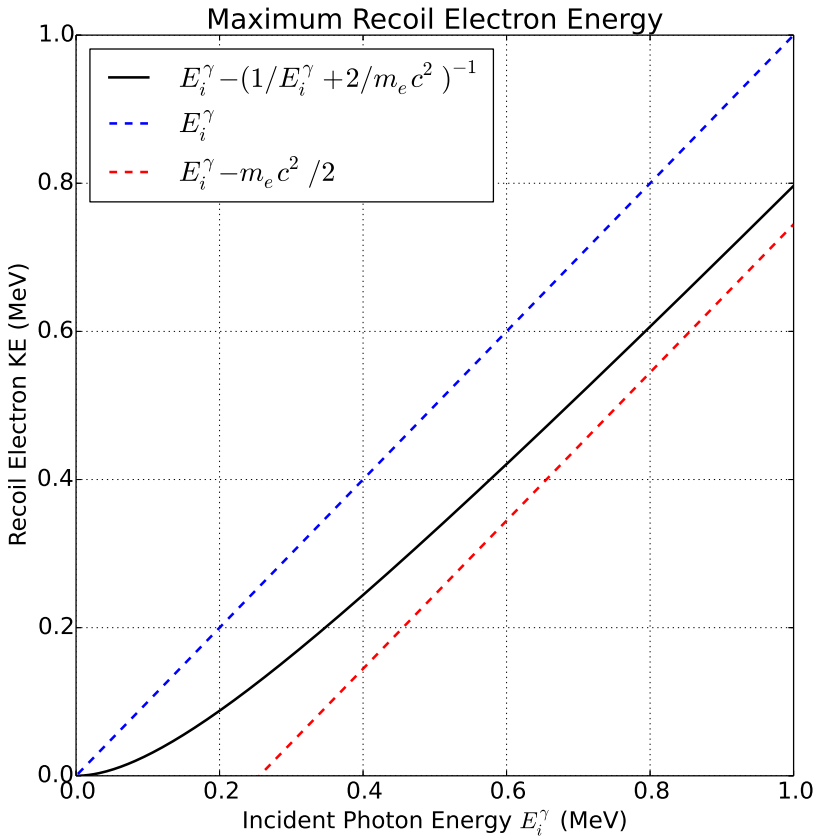

Figure S9: Compton Scattering – the incoherent scattering of photons off of atomic electrons – is the dominant energy loss mechanism for photons in carbon (*e.g.* plastic scintillator) for photons with energy between roughly 10 keV and 10 MeV. It is straightforward to calculate the relationship between the photon energy loss and the photon scattering angle θ: $\frac{1}{E_f^\gamma} - \frac{1}{E_i^\gamma} = \frac{1}{m_e c^2}(1 - \cos\theta)$ where E_i^γ and E_f^γ are the initial and final photon energies, m_e is the mass of the electron and c is the speed of light. The largest momementum transfer to the electron occurs when the photon is back-scattered $\theta = 180°$. In this case the electron kinetic energy T_{max}^e is given by $T_{max}^e = E_i^\gamma - \left(\frac{1}{E_i^\gamma} + \frac{2}{m_e c^2}\right)^{-1} \approx E_i^\gamma - \frac{m_e c^2}{2} = E_i^\gamma - 0.25 MeV$ in the limit $(E_i^\gamma \to \infty)$. The figure shows the maximum Compton electron kinetic energy versus incident photon energy, along with the incident photon (dashed blue) and asymptotic limit (dashed red) curves.

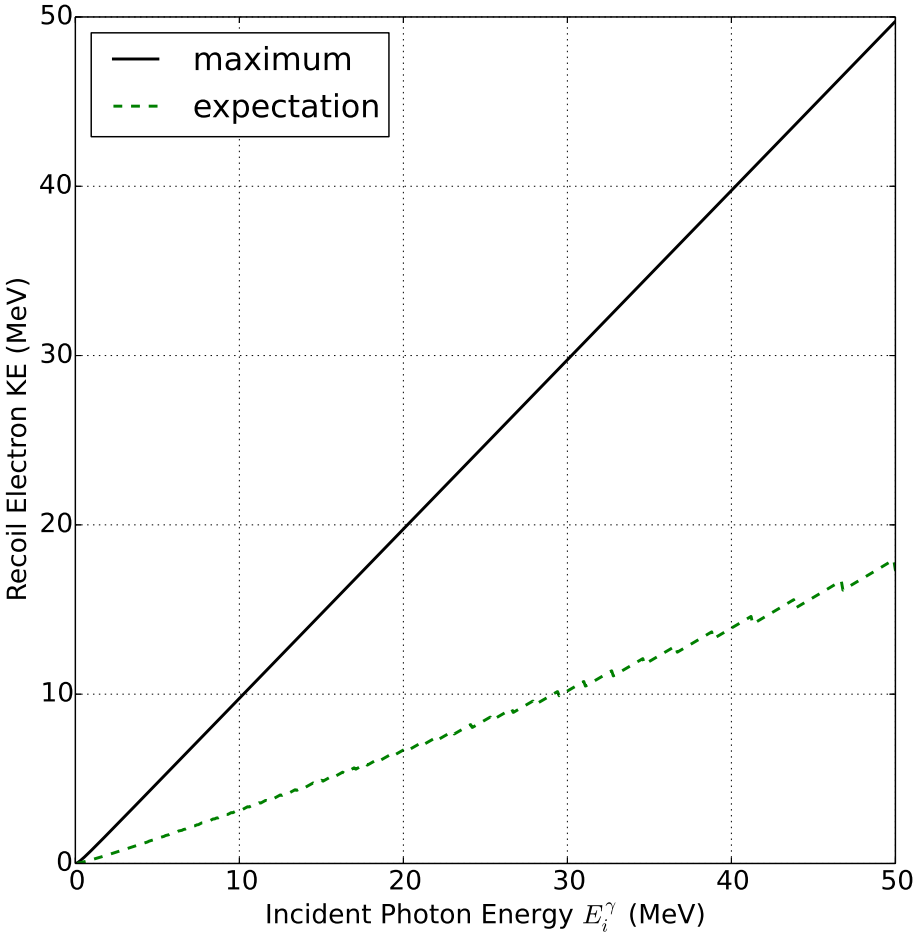

Figure S10: The angular distribution for Compton Scattering is described by the *Klein-Nishina Differential Cross Section* (O. Klein and Y. Nishina, Z. Phys. **52** 853 and 869 (1929)) for photons scattered off of a single free electron. Rather than being likely to back scatter, the photon angular distribution is increasingly forward peaked as the photon energy increases. Here, we compare the electron kinetic energy vs. incident photon energy for the backscatter condition of Figure S9 (solid black curve, constituting the maximum fractional energy transfer) with the expected electron energy when the angular scattering distribution (grazing incidence) is taken into account. Electrons of a given kinetic energy are most likely to have been produced by photons roughly three times more energetic than for the backscatter condition.

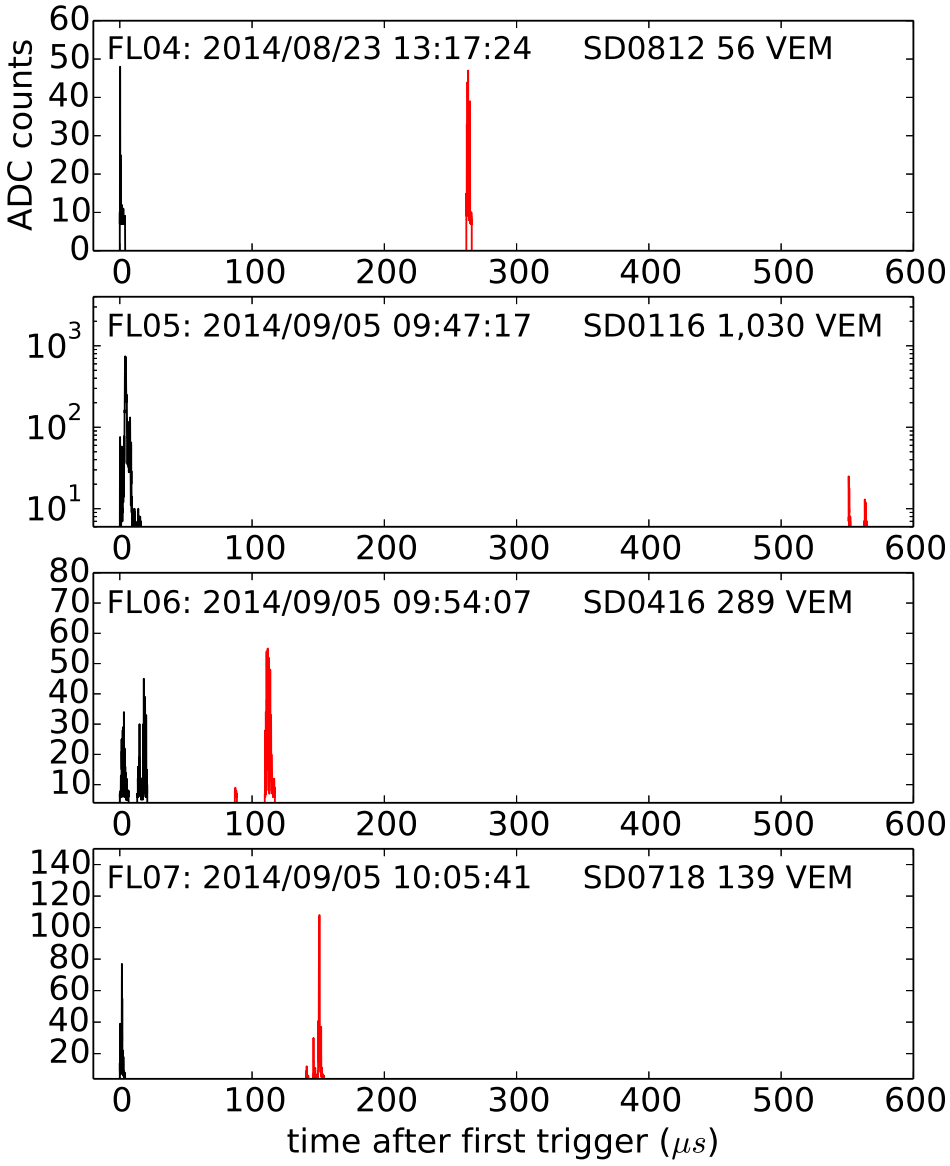

Figure S11: Compare Figure 5 of main text. Combined TASD waveform plots for Slow Antenna Correlated flashes FL04-FL07. Each trigger is colored individually. Triggers 1 and 2 are colored in black and red, respectively.

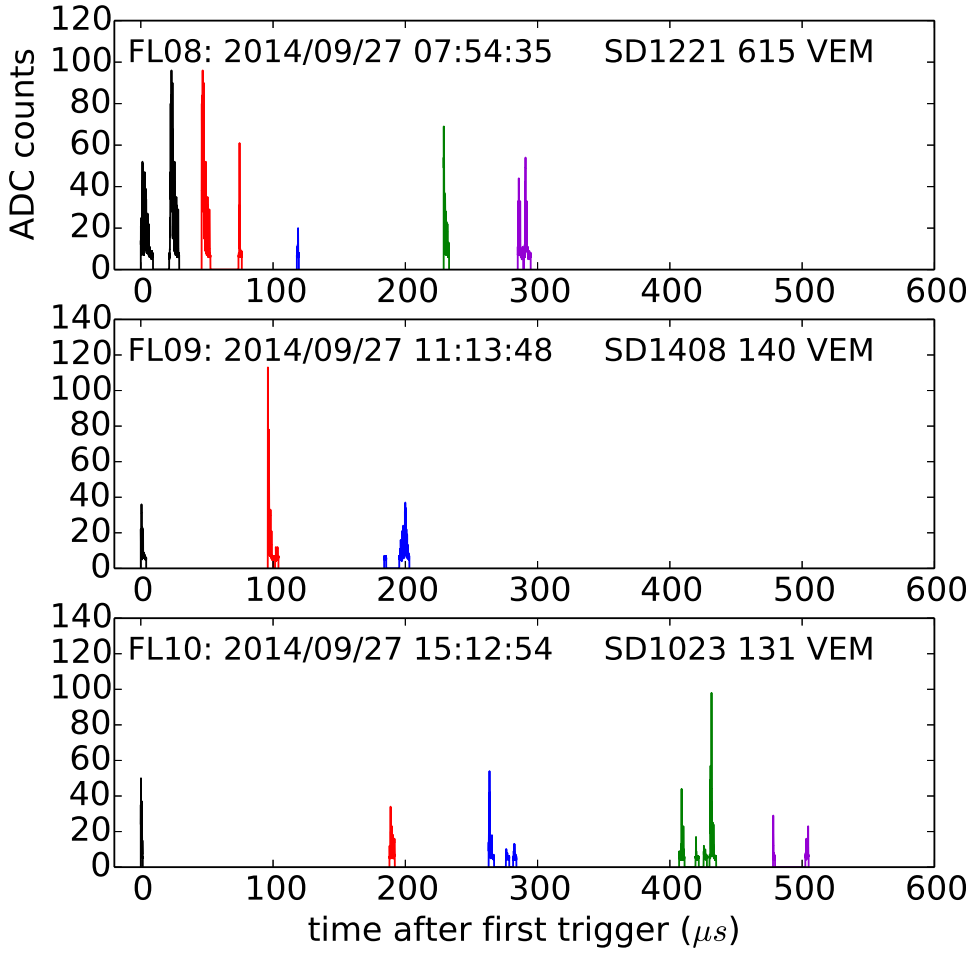

Figure S12: Compare Figure 5 of main text. Combined TASD waveform plots for Slow Antenna Correlated flashes FL08-FL10. Each trigger is colored individually. Triggers 1 through 5 are colored in black, red, blue, green and violet in sequence.

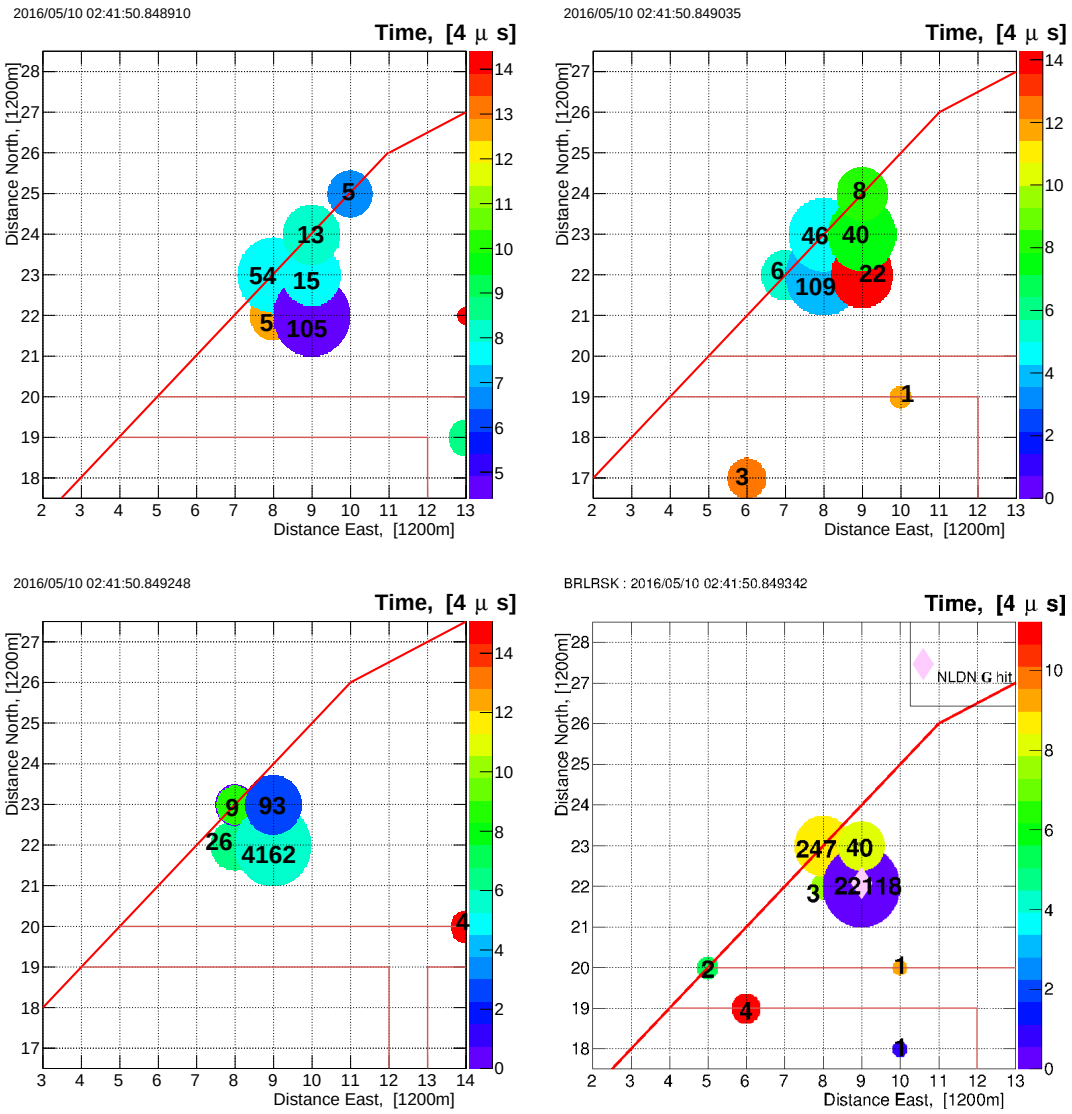

Figure S13: TASD footprints of four consecutive triggers collected on 10 May 2016 at 02:41:50 UTC. See discussion of FL03 in the main text. The energetic leader propagated rapidly to ground, resulting in a -94.1 kA cloud-to-ground stroke occurring 26 μs after the start of the fourth trigger. The NLDN location of this stroke is shown in the lower right panel only. This stroke struck the ground 78 m from TASD 0922 and produced minor RF interference in its waveform as discussed in the text.

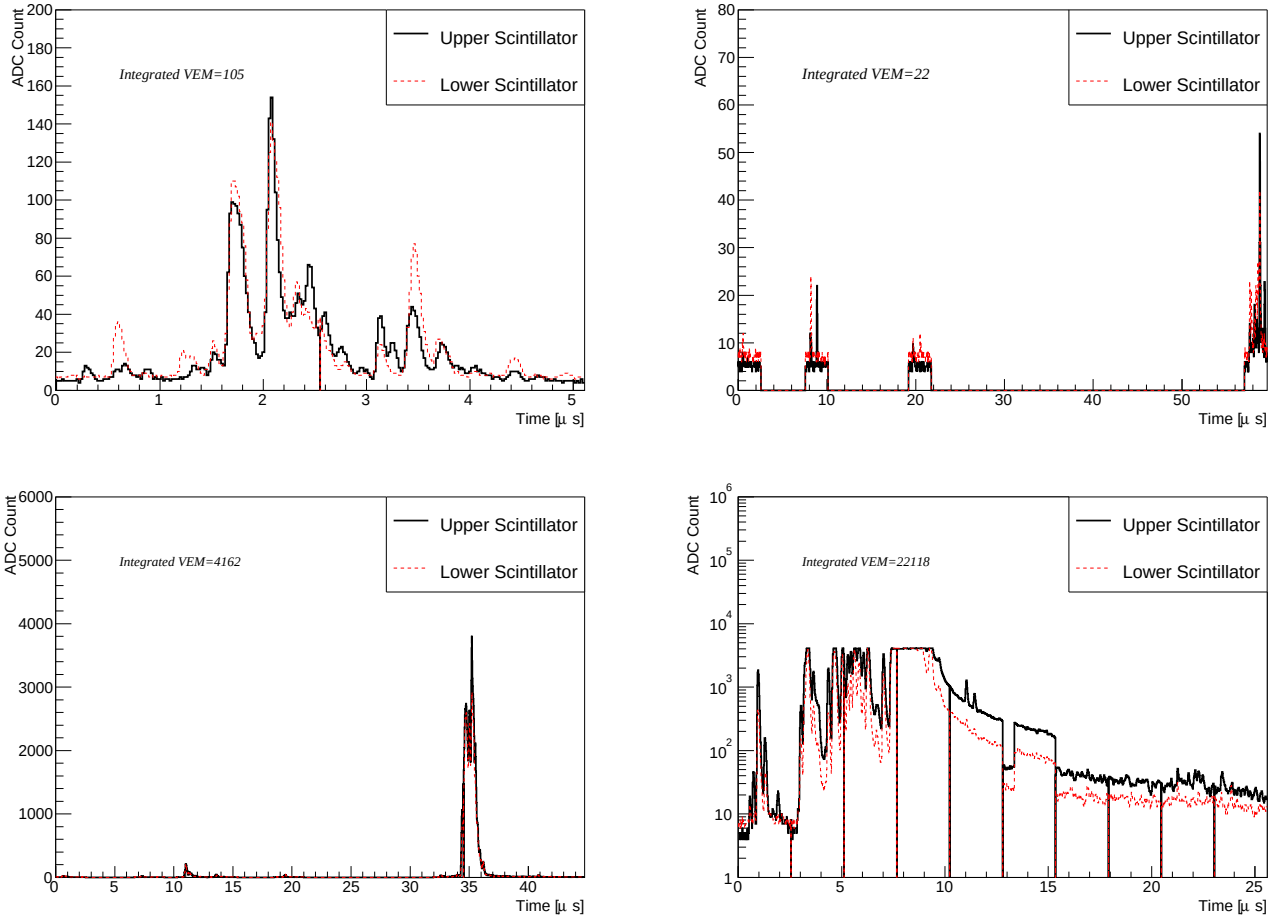

Figure S14: TASD 0922 FADC waveforms for the four consecutive triggers of Figure S13. See discussion of FL03 in the main text. A -94.1 kA cloud-to-ground stroke occurring 26 μs after the start of the fourth trigger (lower right panel, here with vertical axis logarithmic) struck the ground 78 m from TASD 0922. This waveform shows evidence for a pedestal (electric ground level) shift as well as abrupt ADC count changes at 13 and 15μs. (Note that vertical lines at 2.56 μs intervals are readout artifacts, here and elsewhere in the paper.)

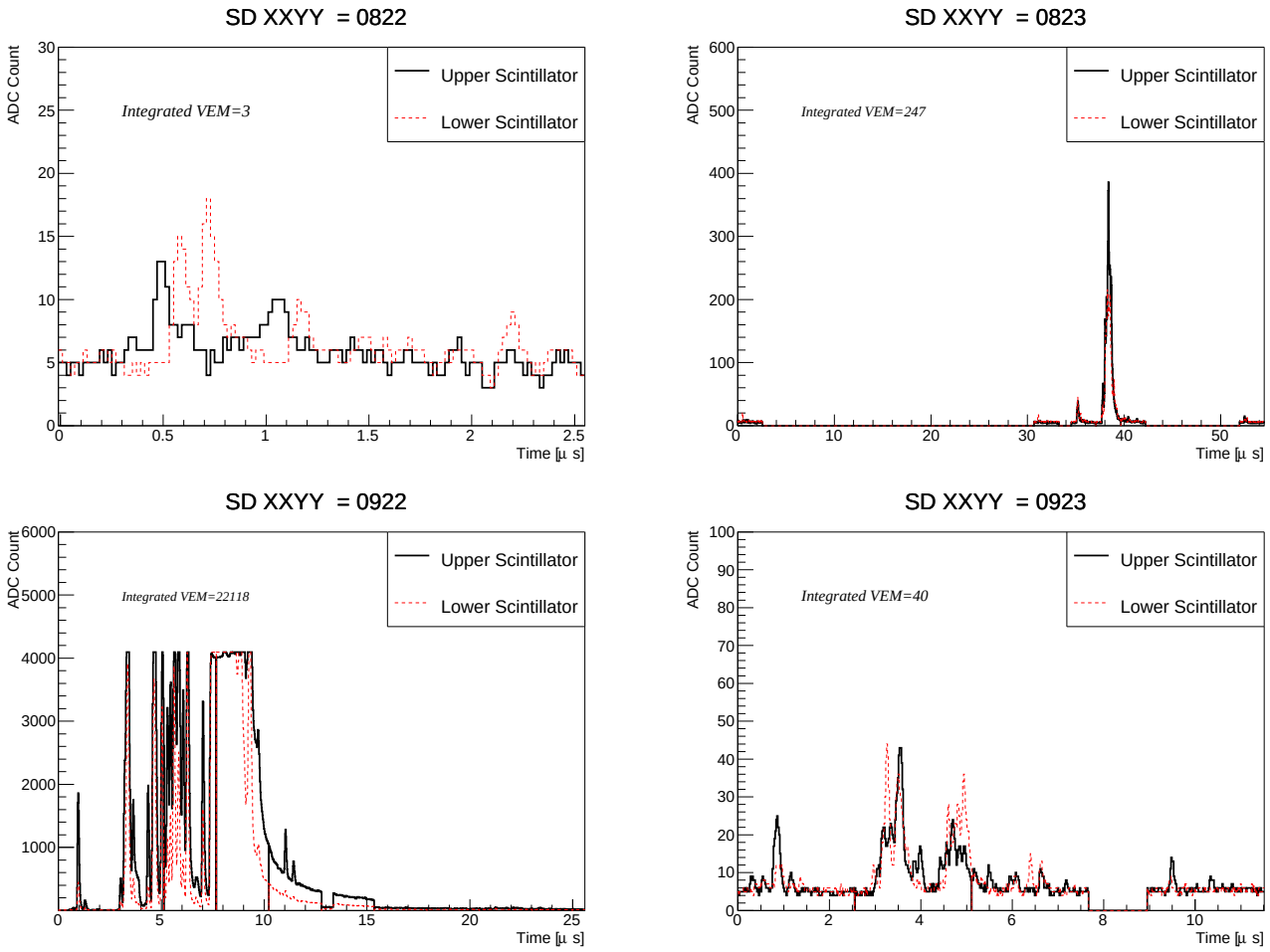

Figure S15: FADC waveforms for the four surface detectors participating in the fourth trigger of FL03. See also Figure S13 and S14, and discussion of FL03 in the main text. A -94.1 kA cloud-to-ground stroke occurring 26 μs after the start of this trigger struck the ground 78 m from TASD 0922 (lower left panel). This waveform shows evidence for a pedestal (electric ground level) shift as well as abrupt ADC count changes at 13 and 15μs.